ELSEVIER

Contents lists available at ScienceDirect

Solid State Sciences

journal homepage: www.elsevier.com/locate/ssscie





Hydrothermal synthesis and structure of ferric molybdates from sodium carbonate solutions

Mahsa Foroughian ^a, Tiffany M.Smith Pellizzeri ^{a,b}, Colin D. McMillen ^a, Kimberly Ivey ^c, Joseph W. Kolis ^{a,*}

- a Department of Chemistry and Center for Optical Materials Science and Engineering Technologies (COMSET), Clemson University, Clemson, SC, 29634, USA
- b Department of Chemistry and Biochemistry, Eastern Illinois University, Charleston, IL, 61920, USA
- ^c Department of Materials Science and Engineering, Clemson University, Clemson, SC, 29634, USA

ARTICLE INFO

Keywords: Hydrothermal Crystal growth Molybdate

ABSTRACT

Several new iron molybdates have been synthesized under hydrothermal conditions at relatively low temperatures (200 °C) to stabilize the Fe³⁺ oxidation state. The mineralizers are all sodium ion based and three new phases were isolated as high quality single crystals from various reaction stoichiometries, Fe(MoO₄)(OH) (I), $Na_{0.15}Fe_2Mo_3O_{12}(H_2O)\cdot 0.25H_2O$ (IIa), and $NaFe(MoO_4)_2(H_2O)$ (III). The structures contain iron oxide octahedra arranged in chains (I), dimers (IIa), and isolated octahedra (III), that are linked by various molybdate oxyanions to form 3-D framework (I), 3-D framework with channels (IIa), and 2-D sheets in their iron molybdate motifs. Both I and III are lightly colored materials containing valence precise Fe³⁺, whereas IIa contains partially occupied Na $^+$ ions in columns within the lattice leading to concomitant valence mixing of Fe $^{2+}$ /Fe $^{3+}$ with a corresponding darker color to the crystal. If sodium ions are not included in the synthesis and instead replaced by smaller Li + ions in the reaction, there is no alkali metal incorporation in the lattice and the resultant compound Fe₂Mo₃O₁₂(H₂O)·0.25H₂O (IIb) is formed. This is isostructural to IIa but without the partially occupied Na + ions in the channels which makes it another valence precise Fe³⁺ compound that is nearly colorless as expected since all transtions are spin forbidden in the high spin $\mathrm{Fe^{3+}}$ case. The role of carbonate as a mineralizer was examined since the reaction is highly acidic (pH \sim 1) in the absence of carbonate, and this does not lead to satisfactory product formation. The carbonate mineralizer increases the pH to 6-6.5, and this pH is maintained throughout the reaction, which does lead to high quality crystal products. Despite its absence in any of the products, the carbonate mineralizer plays an additional important (albeit unknown) role in the synthesis, because if simple hydroxide is used to increase the pH to 6-6.5, the resultant products are much lower in quality and yield.

1. Introduction

Ferric ions (Fe³⁺) display a wide range of interesting chemical and physical behavior in crystalline lattices. Iron(III) sulfates, for example, possess a very rich chemistry and magnetism [1,2]. A transition metal analog to the sulfate anion is the molybdate anion, $(MoO_4)^2$, which is also tetrahedral and magnetically silent, and displays versatile coordination behavior. The *d*-orbital building blocks of molybdenum provide an interesting direct alternative to the sulfates as in Fe₂(MoO_4)₃ [3,4] since the magnetic coupling can be dominated by superexchange through the oxyanion building block [5,6]. Ferric molybdates containing alkali metal cations in the lattice also posses extensive structural and magnetic behavior. In particular the $AFe(MoO_4)_2$ system (A = K, Rb, Cs)

has a trigonal structure with a very complex magnetic phase diagram including multiferroic phases induced by chiral magnetism [7–13]. The material also displays considerable structural sensitivity to pressure and temperature [14–16]. In addition to the interesting magnetic behavior the alkali metal ferric molybdates also display potential uses in battery applications [17–20] and catalysis [21,22]. There are many other structural variations in the alkali ion ferric molybdate phase space suggesting that the descriptive chemistry is still not complete and that additional exploratory phase development is worthwhile [23–32].

Previous work in our group demonstrated that the hydrothermal approach works well for the synthesis of new metal molybdates. Most of that work was done at higher temperatures (500-600 °C) and explored divalent transition metal ions [33,34]. In the case of iron, the divalent

^{*} Corresponding author. 485 H.L. Hunter Laboratories, Clemson, SC, 29634, USA. *E-mail address*: kjoseph@clemson.edu (J.W. Kolis).

oxidation state appears to be somewhat more stable than the trivalent state at these elevated temperatures without addition of an external oxidant. Our goal is to begin studies at lower temperatures (200–220 °C) to identify new alkali ferric molybdates and eventually try to determine the thermal stability zone of the ferric state. In this paper we describe our initial attempts to specifically focus on the use of sodium ions as the alkali building block. We find a number of interesting new phases can be isolated containing the ferric ion, along with a variety of hydroxylated and hydrated building units in the lattice. A systematic variation of mineralizer suggests that carbonate is very useful assisting in crystal growth of the products. A number of new materials are isolated and characterized herein. The influence of carbonate, pH, and hydroxylated species toward the iron molybdate chemical phase space is discussed.

2. Experimental section

2.1. General hydrothermal synthesis and crystal growth of novel iron molybdates

The hydrothermal reactions were carried out in Parr 4749 acid digestion vessels. These Teflon-lined autoclaves containing chemical reagents (\sim 2 g total) and deionized water (10 mL) were heated at 200 °C for 3–5 days. After gradually cooling the autoclaves to room temperature, the mixture of the products was washed with deionized water and dried. The chemicals used in this study were used as received from the supplier: sodium carbonate (Mallinckrodt, 99.997 %), lithium carbonate (Sigma-Aldrich, 99+%), sodium hydroxide (Alfa Aesar, 99.99+%), iron (II) chloride tetrahydrate (Alfa Aesar, 98 %) molybdenum(VI) oxide (Alfa Aesar, 99.5 %), sodium chloride (VWR, 99.997 %), and lithium chloride (Sigma-Aldrich, 99 %).

2.1.1. Synthesis of Fe(MoO₄) OH (I)

Single crystals of Fe(MoO₄)OH (I) were synthesized from mixture of iron(II) chloride tetrahydrate (0.422 mmol, 0.084 g), molybdenum(VI) oxide (0.422 mmol, 0.061 g), and sodium carbonate (0.422 mmol, 0.044 g) in a 1:1:1 molar ratio with 10 mL of 3 M sodium chloride under the above hydrothermal conditions for three days. Once the mixture of products was filtered, light green square platelike crystals were identified as $Fe_2(MoO_4)_3$ [35–38] (major product), and orange blocky crystals were identified as I (minor product) by single crystal X-ray diffraction. The starting and final pH values of the mixture of chemicals were measured by pH test paper strips, and recorded 6.5 and 6, respectively.

2.1.2. Synthesis of $Na_{0.15}Fe_2Mo_3O_{12}(H_2O)\cdot 0.25H_2O$ (IIa)

Single crystals of $Na_{0.15}Fe_2Mo_3O_{12}(H_2O)\cdot 0.25H_2O$ (IIa) were prepared using the same initial reagents and conditions as in I, while using twice the amount of sodium carbonate. Iron(II) chloride tetrahydrate (0.422 mmol, 0.084 g), molybdenum(VI) oxide (0.422 mmol, 0.061 g), and sodium carbonate (0.844 mmol, 0.088 g) were used in a 1:1:2 molar ratio with 10 mL of 3 M sodium chloride as the mineralizer. The mixture of products was filtered after five days. The reaction yielded light green square plate crystals of $Fe_2(MoO_4)_3$, and dark green tabular crystals of IIa as the major phase, identified by single-crystal X-ray diffraction. The starting and final pH values of the reaction mixture were measured by pH test paper strips, and recorded 6.5 and 6, respectively.

2.1.3. Synthesis of $Fe_2Mo_3O_{12}(H_2O) \cdot 0.25H_2O$ (IIb)

Single crystals of $Fe_2Mo_3O_{12}(H_2O)\cdot 0.25H_2O$ (IIb) were prepared using the same initial reagents, conditions, and mole ratios as IIa, except using lithium carbonate and lithium chloride instead of sodium carbonate and sodium chloride as mineralizers. Iron(II) chloride tetrahydrate (0.422 mmol, 0.084 g), molybdenum(VI) oxide (0.422 mmol, 0.061 g), and lithium carbonate (0.844 mmol, 0.062 g) were used in a 1:1:2 molar ratio with 10 mL of 3 M lithium chloride as the mineralizer. The mixture of products was filtered after five days. The reaction yielded light green square plate crystals of $Fe_2(MoO_4)_3$, and yellow tabular

crystals of **IIb** as the major phase, identified by single-crystal X-ray diffraction. The starting and final pH values of the mixture of chemicals were measured by pH test paper strips, and recorded 6.5 and 6, respectively.

2.1.4. Synthesis of NaFe(MoO₄)₂(H₂O) (III)

Single crystals of NaFe(MoO₄)₂(H₂O) (III) were obtained using the same initial reagents and conditions as in I, with a modified mole ratio. Iron(II) chloride tetrahydrate (0.422 mmol, 0.084 g), molybdenum(VI) oxide (0.844 mmol, 0.122 g), and sodium carbonate (0.844 mmol, 0.089 g) were used in a 1:2:2 molar ratio with 10 mL of 3 M sodium chloride as the mineralizer. After three days, the products were filtered from the Teflon liner which yielded yellow needle shaped crystals identified as III through single-crystal X-ray diffraction as the main product, accompanied by a secondary product of Fe₂O₃. The starting and final pH values of the mixture of chemicals were measured by pH test paper strips, and recorded 6.5 and 5.5, respectively.

2.2. X-ray crystallography

The single-crystal X-ray data for structures of Fe(MoO₄)(OH) (I), $Na_{0.15}Fe_2Mo_3O_{12}(H_2O)\cdot 0.25H_2O$ (IIa), $Fe_2Mo_3O_{12}(H_2O)\cdot 0.25H_2O$ (IIb), and NaFe(MoO₄)₂(H₂O) (III) were collected at room temperature from well-formed single crystals of each compound using a Bruker D8 Venture diffractometer (Mo K α radiation, $\lambda = 0.71073$ A, Photon 100 detector). The data were collected from ϕ and ω -scans with 0.5° frame width. The APEX3 software was used to index and process the data [39]. The SHELXTL software was used to determine the space group (XPREP) of structures I-III, with structure solution by intrinsic phasing (SHELXT) and subsequent refinement by full-matrix least-squares techniques on F² (SHELXL) [40]. Complementary characterization of the elemental composition by energy-dispersive X-ray analysis and infrared spectroscopy were used in conjunction with bond valence sum analysis to reach the appropriate structural model. All non-hydrogen atoms were refined anisotropically, while hydrogen atoms attached to oxygen atoms of hydroxide groups or water molecules were identified from the difference electron density map and their positions refined using appropriate distance fixing restraints. After establishing the framework structure of Fe₂Mo₃O₁₂(H₂O)·0.25H₂O in the refinement of IIa, additional residual electron density of 3.39 $e^{-1} \mathring{A}^3$ was found in the channels of the structure. Upon acquisition of EDX data and in consideration of its local environment, this was subsequently modeled as a partially occupied sodium ion at 15 % occupancy with good anisotropic displacement parameters. The largest remaining difference electron density peak was then found to be $1.10 e^{-1} \mathring{A}^3$. In the case of **III**, refinement in the correct absolute structure is supported by the resulting Flack parameter of 0.05 (3). A summary of the crystallographic data is provided in Table 1, while selected interatomic distances and the corresponding bond valence sum analyses are given in Table 2. The structures are deposited with the joint CCDC/FIZ Karlsruhe deposition service, and are available upon quoting deposition numbers CSD 2244227-2244231.

2.3. Spectroscopic characterization

The infrared spectra were collected using pure single crystal samples of **I**, **IIa**, **IIb**, and **III**. To attain the spectra, a Thermo-Nicolet 6700 FTIR equipped with a Thermo-Nicolet Continuum FTIR microscope and a MCT/A detector was used over the range of 650–4000 cm⁻¹. A well formed single crystal of each compound was separately rolled out on a ZnSe plate, and 16 scans of the sample were used to collect the IR spectra.

Table 1 Crystallographic data for ferric molybdates I-III.

	I	IIa	IIb	III
Empirical Formula	Fe(MoO ₄)(OH)	$Na_{0\cdot15}Fe_2Mo_3O_{12}(H_2O)\cdot 0.25H_2O$	Fe ₂ Mo ₃ O ₁₂ (H ₂ O)·0.25H ₂ O	NaFe(MoO ₄) ₂ (H ₂ O)
F. W. (g/mol)	232.80	617.49	614.04	416.73
Crystal System	Monoclinic	Triclinic	Triclinic	Orthorhombic
Space group	C2/c	P-1	P-1	$P2_12_12_1$
a (Å)	7.9318(12)	6.8964(5)	6.8909(2)	5.6876(4)
b (Å)	7.5494(9)	8.4333(5)	8.4302(3)	8.9328(7)
c (Å)	7.6107(8)	9.8597(7)	9.8001(3)	15.8985(13)
α (°)	90	94.489(3)	94.5958(13)	90
β (°)	120.188(4)	109.654(2)	109.3530(11)	90
γ (°)	90	90.822(3)	90.7171(12)	90
Volume (Å ³)	393.92(9)	537.86(6)	534.95(3)	807.74(11)
Z	4	2	2	4
D _{calcd} (g/cm ³)	3.925	3.813	3.812	3.427
μ , mm ⁻¹	6.756	6.109	6.136	4.902
Crystal Size (mm)	$0.07\times0.10\times0.12$	$0.05\times0.05\times0.02$	$0.10\times0.08\times0.04$	$0.18\times0.02\times0.02$
2θ range,°	4.02-28.29	2.42-27.17	2.21-27.16	3.43-25.70
Reflns coll./indep.	3299	12,416	20,549	10,881
Independent reflns	497	2370	2363	1529
No. of parameters	36	189	185	124
R indices (observed data)[a,b]	$R_1 = 0.0377 \text{ w} R_2 = 0.0996$	$R_1 = 0.0230 \text{ w} R_2 = 0.0546$	$R_1 = 0.0202 \text{ w} R_2 = 0.0445$	$R_1 = 0.0274 \text{ w} R_2 = 0.0475$
R indices (all data) [a,b]	$R_1 = 0.0402 \text{ w} R_2 = 0.1019$	$R_1 = 0.0286 \text{ w} R_2 = 0.0590$	$R_1 = 0.0261 \text{ w} R_2 = 0.0482$	$R_1 = 0.0340 \text{ w} R_2 = 0.0492$
Goodness of fit	1.242	1.100	1.171	1.064

3. Results and discussion

3.1. Synthesis and phase description

The main goal of this work was to explore the synthesis of novel iron molybdates using low-temperature hydrothermal reaction conditions. A critical component of this study is the role of carbonate ions in the formation of new iron molybdates. All reactions producing compounds I, IIa, IIb, and III were performed in the presence of carbonate mineralizers, and specific product formation (Fig. 1) appears to be sensitive to parameters such as reaction stoichiometry and pH as well as the concentration of the carbonate mineralizer. This occurs even though the carbonate ion itself is not present in any of the crystallized products. Considering the reaction stoichiometry, compound I, Fe(MoO₄)(OH) formed from a 1:1:1 reaction of FeCl₂·4H₂O + MoO₃ + Na₂CO₃ in 3 M NaCl, while compound IIa, $Na_{0.15}Fe_2Mo_3O_{12}(H_2O)\cdot 0.25H_2O$, formed from the 1:1:2 reaction of $FeCl_2 \cdot 4H_2O + MoO_3 + 2Na_2CO_3$ in 3 M NaCl. Compound III, NaFe(MoO₄)₂(H₂O) formed upon further increasing the amount of MoO₃ to create a 1:2:2 reaction of FeCl₂·4H₂O + 2MoO₃ + 2Na₂CO₃ in 3 M NaCl. In this way the presence of additional MoO₃ in the reactions is generally translated to the resulting products. The ${\rm Fe}^{2+}$ ions in the initial reactants are oxidized to \mbox{Fe}^{3+} during these reactions. There are several potential sources of iron ion oxidation. One is the presence of air in the aqueous fluid and in the headspace of the reaction vessel that can supply some O₂. In addition, the normal Fe²⁺/Fe³⁺ equilibrium in water, $Fe^{2+} + H_2O \Leftrightarrow Fe^{3+} + OH^- + 1/2H_2$, is undoubtedly supported by the relatively high ionic concentration in the fluid. The systematic inclusion of Fe³⁺ into the crystalline product will continue to drive the equilibrium until the reaction is complete.

Transition metal chloride solutions are generally acidic solutions, but the addition of the carbonate mineralizers generates a more basic pH in the solution. None of the products I-III formed from such highly acidic reactions of FeCl₂·4H₂O + xMoO₃ + 3 M NaCl, where carbonate was not included (initial pH \sim 5.5, final pH after the reaction period \sim 1). In those reactions light green crystals of Fe₂(MoO₄)₃ formed as the main product along with Fe₂O₃. When Na₂CO₃ was added to the reaction in equimolar quantities to FeCl₂·4H₂O, the resulting solution was more alkaline, exhibiting an initial pH of 6-6.5, and a pH of 5.5-6 after completion of the hydrothermal reaction. These conditions led to the formation of I-III in addition to Fe₂(MoO₄)₃ and Fe₂O₃. In subsequent experiments, sodium hydroxide (1 M solution) was used instead of sodium carbonate to adjust the pH to the same starting pH of \sim 6–6.5. In these reactions in the absence of carbonate, the yields and sizes of the products I and II were reduced significantly while compound III was not formed at all, and the final pH of the reaction was again highly acidic at \sim 1–1.5. The main product of all comparable reactions involving sodium hydroxide instead of sodium carbonate was again Fe₂(MoO₄)₃. It may be that the buffering effect of the carbonate ions better stabilizes the pH during the course of the reaction period and leads to the formation of the high-quality products we observe.

3.2. Comment on the crystal structure of $Fe_2(MoO_4)_3$

The pale yellow green compound Fe₂(MoO₄)₃ may be considered a "parent" compound in these iron molybdate systems. In our case it invariably occurs in these hydrothermal reactions and can be easily separated from the products of interest. The compound itself is of considerable significance as it displays a unique case of ferrimagnetism which has been analyzed in detail [3,4]. There has been some debate in the literature regarding its structure and given the importance of the structure to the analysis of its magnetic behavior considerable effort has been taken to establish its structure. The original report of the crystal structure of a hydrothermally prepared sample reported the structure in the centrosymmetric space group $P2_1/a$, but raised the possibility of a solution very close to the orthorhombic lattice of Al₂(WO₄)₃ [35]. A ferroelastic transition between monoclinic and orthorhombic structure types has been observed around 500 °C for Fe₂(MoO₄)₃ [36]. A subsequent detailed structural analysis was performed on a flux grown single crystal that suggested the structure adopts the acentric monoclinic space group P2₁ [37]. Concurrent with that work, a structural analysis using a crystal from a high temperature (460 °C) hydrothermal synthesis led to a satisfactory refinement in $P2_1/a$, coupled with the absence of second harmonic generation, and demonstrated that the intensity measurements that would suggest space group P21 could be attributed to crystal twinning [38]. The subsequent magnetic, neutron, and Mössbauer studies employed this centrosymmetric P2₁/a structure and realized satisfactory results [3,4]. Given the prevalence of Fe2(MoO4)3 as a product in the present study, we took the opportunity to verify the structure of Fe₂(MoO₄)₃ obtained from low temperature hydrothermal fluids. It refined very well in the standard $P2_1/c$ setting for the

 $[\]label{eq:resolvent} \begin{array}{l} ^{\rm a} \ R_1 = \Sigma \big| \big| F_{\rm o} \big| - \big[F_{\rm c} \big| \big| / \Sigma \big| F_{\rm o} \big|. \\ ^{\rm b} \ w R_2 = \big\{ \Sigma \ [w \ (F_{\rm o}^2 - F_{\rm c}^2)^2 \big] / \Sigma [w F_{\rm o}^2]^2 \big\}^{1/2}. \end{array}$

Table 2 Selected interatomic distances (Å) and bond valence sums (valence units) for ferric molybdates I-III. Bond valence parameters of 1.759 (Fe $^{3+}$), 1.734 (Fe $^{2+}$), 1.907 (Mo $^{6+}$), and 1.803 (Na $^+$) were used in the bond valence sum (b.v.s.) calculations (accessed from https://www.iucr.org/resources/data/dataset s/bond-valence-parameters).

I		IIa		IIb	
Fe1–O1 \times 2	2.029	Fe1-O3	1.921(3)	Fe1-O3	1.914(3)
$Fe1O2\times2$	(5) 1.997 (5)	Fe1–O7	1.942(3)	Fe1-O7	1.939(3)
$\text{Fe1-O3} \times 2$	1.9797 (19)	Fe1–O1	2.008(3)	Fe1–O1	2.013(3)
Σ (b.v.s.)	3.11	Fe1–O2	2.017(3)	Fe1–O2	2.018(3)
Mo1-O1 ×	1.740	Fe1–O10 Fe1–O6	2.030(3) 2.030(3)	Fe1–O10 Fe1–O6	2.028(3) 2.035(3)
2	(5)	101-00	2.030(3)	101-00	2.033(3)
Mo1–O2 × 2	1.754 (4)	Σ (b.v.s.)	3.22 Fe ³⁺ (3.01 Fe ²⁺)	Σ (b.v.s.)	3.23 Fe ³⁺ (3.02 Fe ²⁺)
Σ (b.v.s.)	6.16		ŕ		ŕ
Ш		Fe2–O2 Fe2–O12	1.968(3) 1.987(3)	Fe2–O2 Fe2–O12	1.949(3) 1.968(3)
Na1–O1	2.255	Fe2-O5	1.990(3)	Fe2-O5	1.986(3)
No.1 (0.10	(6)	Fe2. 00	1 007(2)	E-2 00	1 000(2)
Na1-O19w	2.276 (7)	Fe2–O9	1.997(3)	Fe2–O9	1.992(3)
Na1-O3	2.385 (8)	Fe2-O4	2.055(3)	Fe2-O4	2.037(3)
Na1-O2	2.418	Fe2-O1	2.120(3)	Fe2-O1	2.111(3)
Na1-O8	(7) 2.498 (7)	Σ (b.v.s.)	2.99 Fe ³⁺ (2.80 Fe ²⁺)	Σ (b.v.s.)	3.10 Fe ³⁺ (2.89
Na1-O5	3.002		Fe ⁻ ')		Fe ²⁺)
Σ (b.v.s.)	(6) 1.16	Mo1-O10	1.744(3)	Mo1-O10	1.743(3)
2 (D.V.S.)	1.10	Mo1-O10 Mo1-O4	1.753(3)	Mo1-O10 Mo1-O4	1.757(3)
Fe1-O6	1.959	Mo1-O7	1.753(3)	Mo1-O7	1.763(3)
Fe1-O5	(7) 1.975	Mo1-O6	1.772(3)	Mo1-O6	1.767(3)
Fe1-O7	(5) 1.993 (6)	Σ (b.v.s.)	6.03	Σ (b.v.s.)	5.99
Fe1–O3	2.004				
Fe1-O2	2.009	Mo2-O13	1.685(3)	Mo2-O13	1.682(3)
Fe1-O4	2.010	Mo2-O5	1.756(3)	Mo2-O5	1.766(3)
Σ (b.v.s.)	3.20	Mo2-O3	1.905(3)	Mo2-O3	1.904(3)
Mo1 O1	1.705	Mo2-O2	1.914(3)	Mo2-O2	1.920(3)
Mo1–O1	(5)	Mo2–O3	2.226(3)	Mo2–O3	2.222(3)
Mo1-O4	1.750 (5)	Mo2–O11w	2.340(3)	Mo2-O11w	2.334(3)
Mo1-O2	1.793 (5)	Σ (b.v.s.)	6.02	Σ (b.v.s.)	6.02
Mo1-O3	1.793 (5)				
Σ (b.v.s.)	5.97	Mo3-O8	1.698(3)	Mo3-O8	1.702(3)
Mo2-O8	1.712	Mo3–O9 Mo3–O12	1.761(3) 1.762(3)	Mo3–O9 Mo3–O12	1.759(3) 1.759(3)
Mo2-O7	(5) 1.756	Mo3-O1	1.844(3)	Mo3-O1	1.844(3)
Mo2-O6	(6) 1.765	Σ (b.v.s.)	5.91	Σ (b.v.s.)	5.91
Mo2-O5	(6) 1.779				
Σ (b.v.s.)	(5) 6.08	Na1–O11w	2.253(15)		
		Na1-O13	2.283(15)		
		Na1-O13	2.424(15)		
		Na1-06	2.476(15)		
		Na1-O11w	2.482(15)		
		Na1-O8 Na1-O10	2.529(15) 2.718(14)		
		Na1-O10 Σ (b.v.s.)	2.718(14) 1.30		
		۵ (۵.۷.۵.)	1.50		

centrosymmetric structure previously reported in the nonstandard $P2_1/a$. The crystal was refined as a pseudo-merohedral twin, a condition that seems inherent to this material [38]. The details are given in the supplementary information, Table S1.

3.3. Crystal structure of Fe(MoO₄)(OH) (I)

One new phase of this reaction series crystallizes as orange block-like crystals with the formula Fe(MoO₄)(OH) (Fig. 2a). The structure contains only one unique Fe³⁺ site and consists of corner shared FeO₆ octahedra units in one-dimensional (1–D) chains propagating along the c-axis (Fig. 2b). The corner-sharing oxygen atom in the FeO₆ chain, O(3), is the OH group in the structure with the hydrogen atom identified from the difference electron density map. The hydroxide group is in a weak bifurcated hydrogen bond to two symmetry-related O(1) atoms (D-H = 0.90(2), D ... A = 3.343(8) Å; H···A = 2.561(19) Å; D-H···A =146.4(3)°). There is one independent tetrahedrally-coordinated molybdenum atom in the structure. These molybdate oxyanions, $(MoO_4)^{2-}$, reinforce the [FeO₆]_n chains by connecting neighboring O(2) atoms of each FeO₆ octahedron along the chain, while also providing connections to two O(1) atoms of two neighboring chains (Fig. 2c). This creates an overall three-dimensional (3-D) iron molybdate structure from the 1-D iron oxide substructure and molybdate tetrahedra. The six-coordinate Fe³⁺ ions exhibit bond lengths to oxygen ranging from 1.9797(19) Å to 2.029(5) Å, averaging 2.002(5) Å, consistent with Fe³⁺ via bond valence sum calculations (Table 2). This further distinguishes the structure type from the simple divalent metal molybdate hydrates such as triclinic Mn(MoO₄)(H₂O) having edge-sharing dimers of manganese oxide octahedra [41], and triclinic Co(MoO₄)(H₂O)_{0.75} [42] and Ni (MoO₄)(H₂O)_{0.7} [43], which are based on Z-shaped tetrameric transition metal oxide building blocks. The simple trivalent metal sulfates Fe(SO₄) (OH) [44] and Fe(SO₄)F [45] are structurally analogous to Fe(MoO₄) (OH), though Fe(MoO₄)(OH) shows a greater disparity in its ratio of a/clattice parameters.

3.4. Crystal structure of $Na_{0.15}Fe_2Mo_3O_{12}(H_2O)\cdot 0.25H_2O$ (IIa) and $Fe_2Mo_3O_{12}(H_2O)\cdot 0.25H_2O$ (IIb)

The compounds $Na_{0.15}Fe_2Mo_3O_{12}(H_2O)\cdot 0.25H_2O$ (IIa) $Fe_2Mo_3O_{12}(H_2O)\cdot 0.25H_2O$ (IIb) represent a new structure type, and fundamentally differ from one another only in partial occupancy of a Na ion in structural voids of IIa compared to IIb. In this way the structure of **IIb** can be used for the majority of the structural description. The iron molybdate network is a complicated framework consisting of three unique molybdenum atoms having two different coordination numbers (two four-coordinate and one six-coordinate), and two unique sixcoordinate iron atoms (Fig. 3a). The iron atoms form edge-shared [Fe₂O₁₀] dimers with Fe-O distances ranging from 1.914(3) Å to 2.111(3) Å, averaging 1.999(3) Å. The two four-coordinate [MoO₄] units link these dimers into iron molybdate slabs in the ab plane. The sixcoordinate molybdenum site, coordinated as [MoO5(H2O)], serves to connect these neighboring slabs along the c-axis (Fig. 3a). These sixcoordinate molybdates also occur as edge-sharing dimers with one another. So an alternative interpretation of the framework can be to describe sheets of edge sharing [Fe₂O₁₀] dimers and [Mo₂O₈(H₂O)₂] dimers in the bc plane (Fig. 3b) that are then linked into the framework by the tetrahedral molybdate groups. The Mo⁶⁺ ion typically appears as four-coordinate tetrahedral (MoO₄)²⁻ in metal oxide structures but sixcoordinate molybdate octahedra (MoO₆)⁶⁻ are also reported in the literature, particularly in condensed oxides such as perovskites and double perovskites [46–48]. The oxidation states of Fe^{3+} and Mo^{6+} at all of their respective sites are supported by the bond valence sums.

The connection of iron and molybdate building blocks generates a 3-D framework containing channels along the b-axis (Fig. 3a). The water molecule coordinated to the six-coordinate molybdenum atom extends into these channels, and the channels also accommodate a partially-

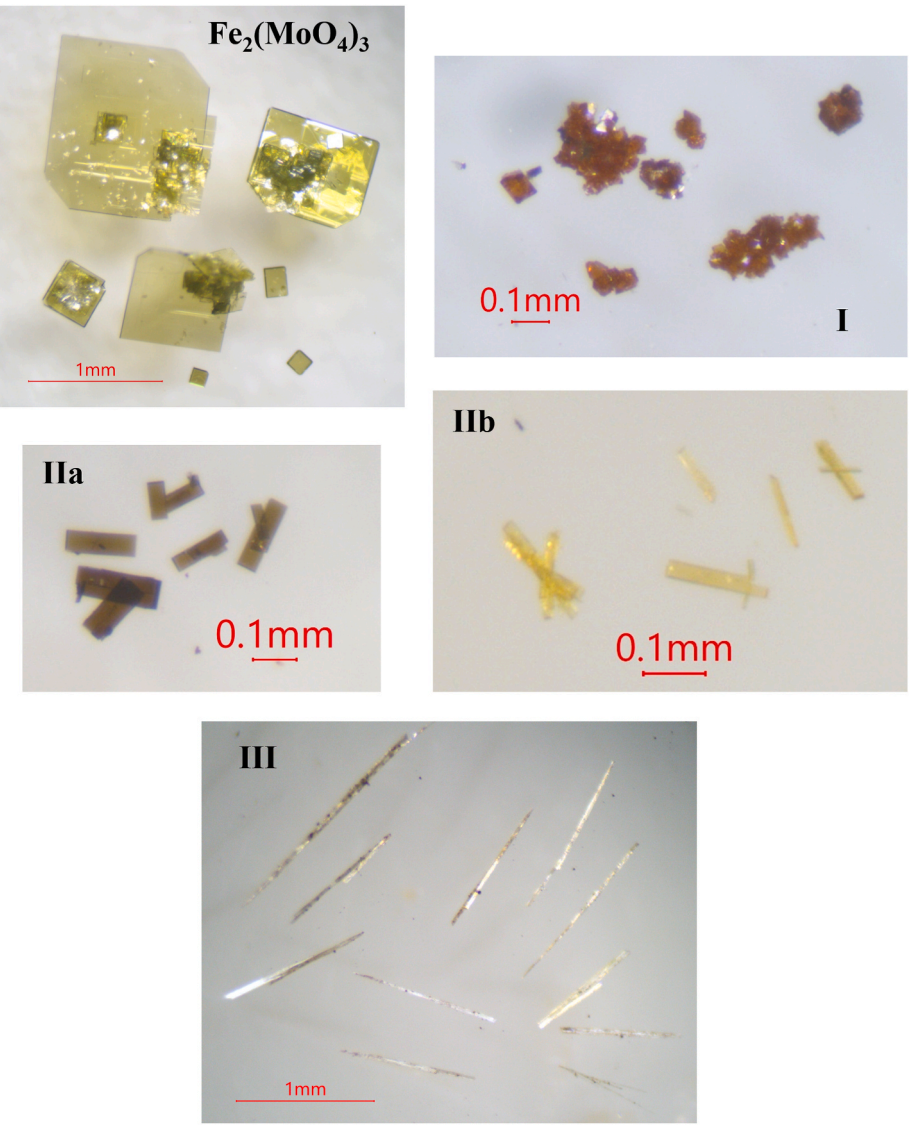


Fig. 1. Optical micrographs of ferric molybdates obtained from low temperature hydrothermal reactions in aqueous carbonate solutions.

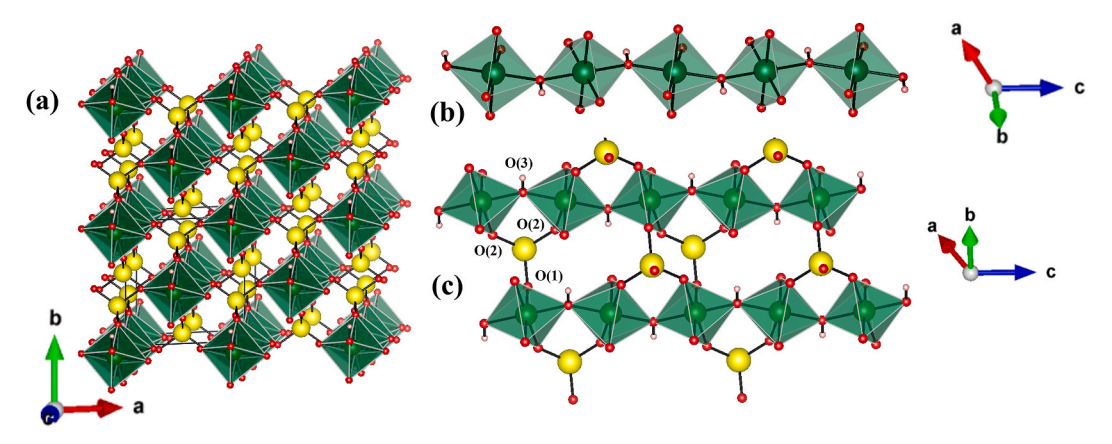


Fig. 2. Structure of Fe(MoO₄)(OH) (I). Iron atoms are shown as green polyhedra, molybdenum atoms as yellow spheres, oxygen atoms as red spheres, and hydrogen atoms as pink spheres. (a) 3-D framework packing viewed off the c-axis. (b) 1-D iron oxide substructure of corner sharing octahedra. (c) Connectivity of neighboring chains through MoO_4 tetrahedra.

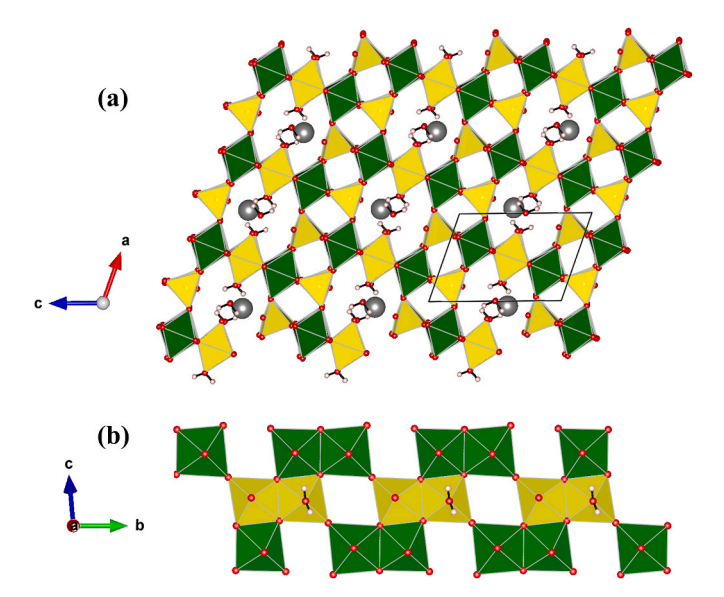


Fig. 3. Structure of IIa/IIb. Iron atoms are shown as green polyhedra, molybdenum atoms as yellow polyhedra, sodium atoms as gray spheres, oxygen atoms as red spheres, and hydrogen atoms as pink spheres. (a) 3-D framework forming a channel structure, viewed off the b-axis, with all channels shown as containing some amount of partially-occupied sodium and non-coordinated water molecules. (b) Connectivity between iron oxide dimers and molybdenum oxide dimers.

occupied, non-coordinated water molecule. In the case of IIa, the channels further accommodate the low-occupancy Na⁺ site, which sits off center in the channel. To test the role of sodium mineralizers and confirm the presence of partial sodium occupancy in structure IIa, we performed a reaction using identical stoichiometry and conditions, but with no sodium (instead using LiCl (3 M)/Li₂CO₃ as mineralizer). That Na-free reaction led to the formation of $Fe_2Mo_3O_{12}(H_2O)\cdot 0.25H_2O$ (IIb) crystals in the exact shape of IIa crystals (long plates) but light yellow instead of dark green in color. A consequence of the partial Na⁺ occupancy in ${\bf Ha}$ is that some of the ${\rm Fe}^{3+}$ must be reduced to maintain charge balance. Typically, all single-valence Fe³⁺ containing crystals occur as yellow, pale orange, or light green colors due to the spin forbidden transitions from the $^6\mathrm{A}_{1\mathrm{g}}$ ground state in the high spin d^5 system. The nearly colorless appearance of IIb suggests that all of the iron atoms are in the +3 oxidation state as they should be in the absence of any extraneous Na⁺ or Li⁺ ions. Therefore, the brownish-dark green color of Na_{0·15}Fe₂Mo₃O₁₂(H₂O)·0.25H₂O crystals is of some support for the mixed-valence iron building blocks. The EDX data of IIa and IIb are essentially identical concerning the heavy elements that are reliably measured, except that the spectrum for IIa indicates a trace amount of sodium from the Kα energy at 1.04 eV, and IIb does not, providing further support for the theory (Supplementary Information, Fig. S1, S2). While sodium is present in trace amounts in IIa, it does not play a significant role in stabilizing the overall iron molybdate lattice shared by IIa and IIb. The partial reduction of Fe^{3+} to Fe^{2+} in IIa may present itself in the longer Fe-O bond lengths at the Fe2 site, averaging 2.020(3) Å in **IIa** versus 2.007(3) Å in **IIb**.

3.5. Crystal structure of NaFe(MoO₄)₂(H₂O) (III)

The compound NaFe(MoO₄) $_2$ (H₂O) (III) crystallizes as pale yellow needles and was refined in the noncentrosymmetric space group $P2_12_12_1$ with a Flack parameter of 0.05(3). Structure III consists of isolated [FeO₆] octahedra bridged by two unique [MoO₄] tetrahedra to form a two-dimensional (2-D) iron molybdate substructure in the ab plane (Fig. 4a). Six [MoO₄] tetrahedra surround each [FeO₆] octahedron, and each [MoO₄] tetrahedron is surrounded by three adjacent [FeO₆]

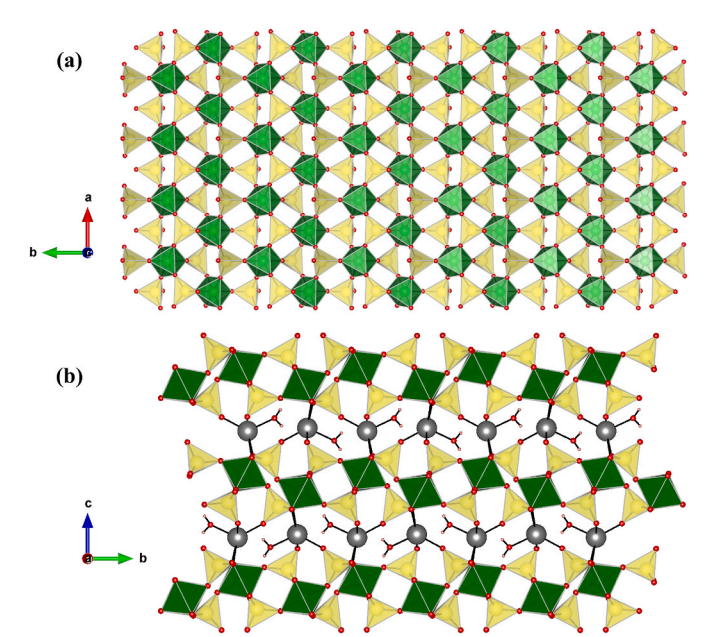


Fig. 4. Structure of NaFe(MoO₄)₂(H₂O) (**III**). Iron atoms are shown as green polyhedra, molybdenum atoms as yellow polyhedra, sodium atoms as gray spheres, oxygen atoms as red spheres, and hydrogen atoms as pink spheres. (a) 2-D iron molybdate substructure viewed along the c-axis. (b) Connectivity of iron molybdate layers by sodium atoms residing between the layers.

octahedra. These iron molybdate layers are connected along the c-axis by sodium atoms (Fig. 4b). Additional vacancies between the sodium ions that connect the layers are occupied by one unique water molecule that is coordinated to the sodium atom at a distance of 2.276(8) Å.

The Fe-O and Mo-O bond lengths are in good agreement with Fe³⁺ and Mo⁶⁺, respectively. The six Fe–O bonds in **III** are distributed over a narrow range, 1.960(7) Å to 2.010(5) Å, averaging 1.992(7) Å, similar to the other Fe³⁺ structures in this study. The sodium ion that connects the layers can be considered as a [NaO₅] polyhedron or a highly distorted [NaO₆] polyhedron, with five close Na–O contacts within the range of 2.255(6) Å to 2.498(7) Å, while the sixth oxygen atom is located 3.002 (6) Å. To our knowledge there are no directly analogous orthorhombic structure types to compound III that are reported. The anhydrous Fe³⁺ structure, NaFe(MoO₄)₂, is reported to crystallize in space group C2/c with a = 9.87 Å, b = 5.31 Å, c = 13.57 Å, $\beta = 90.4^{\circ}$, with R1 = 0.094 [49]. While that structure has the topological similarity of iron molybdate layers separated by sodium ions along the longest crystallographic axis, the layers in III are corrugated with respect to the iron atoms which also results in greater tilting of the terminal Mo-O bonds relative to the c-axis in III versus NaFe(MoO₄)₂. This may be necessary to accommodate the additional water molecule between the layers in III. Accordingly, **III** features a somewhat larger unit cell volume of 807.74(11) Å³ compared to 711.18 Å³ in NaFe(MoO₄)₂. Unlike the situation for I, there is not a directly analogous sodium iron sulfate composition to III, as the most obvious stoichiometric comparison, NaFe(SO₄)₂(H₂O)₆, contains numerous coordinated water molecules that interrupt the formation of any 2-D iron sulfate substructure [50].

3.6. Infrared spectra of I, IIa, IIb and III

The infrared active regions for molybdate groups, hydroxide groups, and water molecules, of **I**, **IIa**, **IIb**, and **III** are shown in Fig. 5. The characteristic Mo–O stretches occur in the region between 1000 and 500 cm^{-1} , including asymmetric stretching modes from 750 cm^{-1} – 900 cm^{-1} , Fe–O–Mo vibrations from \sim 940 cm⁻¹– 970 cm^{-1} , and accentuated bands at 750 cm^{-1} in **IIa** and 740 cm^{-1} in **IIb** from the hexacoordinated molybdate blocks in those structures [51,52]. All four new compounds

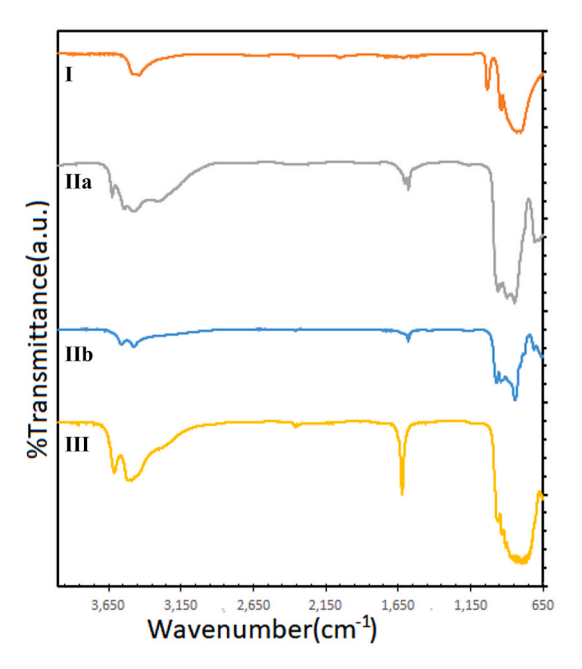


Fig. 5. Infrared spectra of I (orange), IIa (gray), IIb (blue), III (yellow).

contain water or hydroxide in various roles in the crystalline lattices, and display the characteristic O–H stretching band at $\sim\!3100\!-\!3700$ cm $^{-1}$. The spectra of Na $_{0.15}$ Fe2Mo3O12(H2O)·0.25H2O (IIa), Fe2Mo3O12(H2O)·0.25H2O (IIb), and NaFe(MoO4)2(H2O) (III) exhibit broader features with multiple constituent bands in this region due to symmetric and asymmetric stretching vibrations of coordinated H2O groups, whereas the coordinated O–H group in Fe(MoO4)(OH) (I) structure displays a sharper peak in the same area at 3440 cm $^{-1}$. Moreover, the H–O–H bending modes of coordinated or lattice H2O in IIa, IIb, and III are clearly shown at $\sim\!1574$ cm $^{-1}$, $\sim\!1578$ cm $^{-1}$, and $\sim\!1622$ cm $^{-1}$, and are useful for distinguishing OH $^-$ from H2O in these structures.

4. Conclusions

In this work we demonstrate that a number of new iron molybates can be synthesized using low temperature (200 °C) hydrothermal conditions. The low temperatures favor the stabilization of Fe³⁺ as well as the presence of OH⁻ and/or H₂O in the lattice, either coordinated to the metal center or within columns in the lattice. The alkali metals in the reactions, in this case primarily Na⁺, can act as a mineralizing species and in some cases are incorporated into the final products to stabilize a particular structure type. The series of compounds isolated here are of differing dimensionality with respect to the iron oxide octahedra and bridging molybdate groups. Compound I features a 1-D iron oxide substructure linked into a framework by the molybdate tetrahedra. The compounds IIa/IIb present iron oxide dimers that are linked into a framework by dimers of molybdate octahedra and molybdate tetrahedra. Compound III forms 2-D iron molybdate sheets where the molybdate tetrahedra link otherwise isolated iron oxide octahedra. In all cases, H₂O or OH⁻ play a critical role in the structure of the products, while sodium plays a role in establishing charge balance, inducing partial reduction of Fe³⁺ in IIa, and providing connectivity of the 2-D iron molybdate sheets in III. We find that when other alkali ions are used instead of sodium an entirely different product profile emerges from the reactions. This chemistry will be the subject of subsequent reports.

The role of carbonate in these syntheses is noteworthy. It is well known that carbonate can play a major role in the mineralization and buffering in a wide range of hydrothermal systems. The topic has been especially well studied in natural geochemical systems. The ion can act as a buffer, a mineralizer or precipitating agent whether it becomes incorporated in the final lattice or not [53,54]. In all cases studied in this report, carbonate is not in the structural framework but does play an important role in both the crystallization and the yield of the materials. The presence of the Fe³⁺ creates an acidic environment in the initial reaction mixture and if carbonate is not used, the solution becomes more acidic throughout the reaction (final pH \sim 1) and compounds I-III do not form well or at all. If carbonate is present then the pH increases to around 6-6.5 and the products form in much better quality and yield in all cases, and a pH of ~6 is maintained. If the pH is artificially adjusted with the addition of NaOH to 6-6.5 at the beginning of the reaction the products again do not form as well, so the carbonate is required throughout the reaction, presumably as a buffer, for optimal product formation. The new ferric molybdates synthesized in this lower temperature hydrothermal regime suggest that, with careful reaction control, a fairly rich synthetic chemistry may be accessible toward the preparation of low-dimensional compounds that may be attractive as unusual magnetic materials.

CRediT authorship contribution statement

Mahsa Foroughian: Investigation, Visualization, Writing - original draft. Tiffany M.Smith Pellizzeri: Investigation, Writing - review & editing. Colin D. McMillen: Data curation, Investigation, Visualization, Writing - review & editing. Kimberly Ivey: Investigation, Writing - review & editing. Joseph W. Kolis: Funding acquisition, Supervision, Writing - review & editing.

Declaration of competing interest

The authors declare that they have no known competing financial interests or personal relationships that could have appeared to influence the work reported in this paper.

Data availability

Data will be made available on request.

Acknowledgment

We are indebted to the National Science Foundation for support of this work (NSF-DMR-1808371 and – 2219129).

Appendix A. Supplementary data

Supplementary data to this article can be found online at https://doi.org/10.1016/j.solidstatesciences.2023.107403.

References

- [1] G.J. Long, G. Longworth, P. Battle, A.K. Cheetham, R.V. Thundathil, D. Beveridge, Study of anhydrous iron (III) sulfate by magnetic susceptibility, Moessbauer, and neutron diffraction techniques, Inorg. Chem. 18 (1979) 624–632.
- [2] J. Majzlan, A. Navrotsky, R. Stevens, M. Donaldson, B.F. Woodfield, J. BoerioGoates, Thermodynamics of monoclinic Fe₂(SO₄)₃, J. Chem. Thermodyn. 37 (2005) 802–809.
- [3] Z. Jirak, R. Salmon, L. Foumes, F. Menil, P. Hagenmuller, Magnetic and Moessbauer resonance investigations of the weak ferrimagnet iron molybdate (Fe₂(MoO₄)₃), Inorg. Chem. 21 (1982) 4218–4223.
- [4] P.D. Battle, A.K. Cheetham, G.J. Long, G. Longworth, Study of the magnetic properties of iron (III) molybdate, by susceptibility, Moessbauer, and neutron diffraction techniques, Inorg. Chem. 21 (1982) 4223–4228.
- [5] W. Geertsma, D. Khomskii, Influence of side groups on 90 superexchange: a modification of the Goodenough-Kanamori-Anderson rules, Phys. Rev. B 54 (1996) 3011
- [6] M.H. Whangbo, H.-J. Koo, D. Dai, Spin exchange interactions and magnetic structures of extended magnetic solids with localized spins: theoretical descriptions on formal, quantitative and qualitative levels, J. Solid State Chem. 176 (2003) 417-481.

- [7] M. Kenzelmann, G. Lawes, A.B. Harris, G. Gasparovic, C. Broholm, A.P. Ramirez, G. A. Jorge, M. Jaime, S. Park, Q. Huang, A. Ya Shapiro, L.A. Demianets, Direct transition from a disordered to a multiferroic phase on a triangular lattice, Phys. Rev. Lett. 98 (2007), 267205.
- [8] L.E. Svistov, A.I. Smirnov, L.A. Prozorova, O.A. Petrenko, L.N. Demianets, A. Ya Shapiro, Quasi-two-dimensional antiferromagnet on a triangular lattice RbFe (MoO₄)₂, Phys. Rev. B 67 (2003), 094434.
- [9] T. Inami, Neutron powder diffraction experiments on the layered triangular-lattice antiferromagnets RbFe(MoO₄)₂ and CsFe(SO₄)₂, J. Solid State Chem. 180 (2007) 2075–2079.
- [10] T. Inami, Y. Ajiro, T. Goto, Magnetization process of the triangular lattice antiferromagnets, RbFe(MoO₄)₂ and CsFe(SO₄)₂, J. Phys. Soc. Jpn. 65 (1996) 2374_2376
- [11] A.J. Hearmon, F. Fabrizi, L.C. Chapon, R.D. Johnson, D. Prabhakaran, S. V. Streltsov, P.J. Brown, P.G. Radaelli, Electric field control of the magnetic chiralities in ferroaxial multiferroic RbFe(MoO₄)₂, Phys. Rev. Lett. 108 (2012), 237201
- [12] J.S. White, Ch Niedermayer, G. Gasparovic, C. Broholm, J.M.S. Park, A.Ya Shapiro, L.A. Demianets, M. Kenzelmann, Multiferroicity in the generic easy-plane triangular lattice antiferromagnet RbFe(MoO₄)₂, Phys. Rev. B 88 (2013), 060409
- [13] A.I. Smirnov, T.A. Soldatov, O.A. Petrenko, A. Takata, T. Kida, M. Hagiwara, A. Y. Shapiro, M.E. Zhitomirsky, Order by quenched disorder in the model triangular antiferromagnet RbFe(MoO₄)₂, Phys. Rev. Lett. 119 (2017), 047204.
- [14] D.P. Kozlenko, S.E. Kichanov, E.V. Lukin, N.T. Dang, L.S. Dubrovinsky, E. A. Bykova, K.V. Kamenev, H.P. Liermann, W. Morgenroth, A.Y. Shapiro, B. N. Savenko, Effect of high pressure on the crystal structure, magnetic, and vibrational properties of multiferroic RbFe(MoO₄)₂, Phys. Rev. B 87 (2013), 014112.
- [15] A.I. Otko, N.M. Nesterenko, L.V. Povstyanyi, Phenomenological approach to structural phase transitions in trigonal double molybdates and tungstates, Phys. Status Solidi A 46 (1978) 577–587.
- [16] A. Gagor, P. Zajdel, D. Többens, The phase transitions in CsFe(MoO₄)₂ triangular lattice antiferromagnet, neutron diffraction and high pressure studies, J. Alloys Compd. 607 (2014) 104–109.
- [17] N. Chen, Y. Yao, D. Wang, Y. Wei, X. Bie, C. Wang, G. Chen, F. Du, LiFe(MoO₄)₂ as a novel anode material for lithium-ion batteries, ACS Appl. Mater. Interfaces 6 (2014) 10661–10666.
- [18] A.M. Tamboli, M.S. Tamboli, P.K. Dwivedi, C.S. Praveen, I. Karbhal, M.V. Shelke, B. Kim, C. Park, B.B. Kale, Engineering microstructure of LiFe(MoO₄)₂ as an advanced anode material for rechargeable lithium-ion battery, J. Mater. Sci. Mater. Electron. 32 (2021) 24273–24284.
- [19] A.M. Tamboli, M.S. Tamboli, C.S. Praveen, P.K. Dwivedi, I. Karbhal, S.W. Gosavi, M.V. Shelke, B.B. Kale, Architecture of NaFe(MoO₄)₂ as a novel anode material for rechargeable lithium and sodium ion batteries, Appl. Surf. Sci. 559 (2021), 149903–9.
- [20] C. Cheng, G. Lai, Supercapacitor behavior of nano-Fe₂(MoO₄)₃, J. Mater. Sci. Lett. 301 (2021), 130246–4.
- [21] G. Hidalgo, M. Tonelli, L. Burel, M. Aouine, J.M.M. Millet, Microwave-assisted hydrothermal synthesis, characterization and catalytic performance of Fe₂(MoO₄)₃ in the selective oxidation of propene, Catal. Today 363 (2021) 36–44.
- [22] A.P.V. Soares, M.F. Portela, A. Kiennemann, Methanol selective oxidation to formaldehyde over iron-molybdate, Catal. Rev. Sci. Eng. 47 (2005) 125–174.
 [23] M. Liu, Y. Zhang, T. Zou, V. Ovidiu Garlea, T. Charlton, Y. Wang, F. Liu, Y. Xie,
- [23] M. Liu, Y. Zhang, T. Zou, V. Ovidiu Garlea, T. Charlton, Y. Wang, F. Liu, Y. Xie, X. Li, L. Yang, B. Li, X. Wang, S. Dong, J.M. Liu, Antiferromagnetism of double molybdate LiFe(MoO₄)₂, Inorg. Chem. 59 (2020) 8127–8133.
- [24] E. Muessig, K.G. Bramnik, H. Ehrenberg, Structural investigation of the Na–Fe– Mo–O system, Acta Crystallogr. B59 (2003) 611–616.
- [25] A. Savina, S.F. Solodovnikov, D.A. Belov, Z.A. Solodovnikova, K.V. Pokholok, S. Stefanovich, B.I. Lazoryak, E.G. Khaikina, New double molybdate Na₉Fe (MoO₄)₆: synthesis, structure, properties, J. Chem. 41 (2017) 5450–5457.
- [26] M. Wierzbicka-Wieczorek, E. Tillmanns, U. Kolitsch, Crystal chemistry and topology of Rb—M^{III} molybdates (M= Fe, Sc, In) and triclinic Rb₂Mo₄O₁₃. Novel building blocks, decorated chains and layers, Z. Kristallogr. 224 (2009) 151–162.
- [27] K.G. Bramnik, E. Muessig, H. Ehrenberg, Preparation, crystal structure, and magnetic studies of Na₃Fe₂Mo₅O₁₆, a new oxide containing Mo₃O₁₃ clusters, J. Solid State Chem. 176 (2003) 192–197.
- [28] M.B. Zapart, W. Zapart, Trigonal double molybdates and tungstates: Ferroelastic phase transitions, in: Perovskites and Other Framework Crystalline Materials, 2021, pp. 327–353. Ch 10.

- [29] T. Namsaraeva, B. Bazarov, D. Mikhailova, N. Kuratieva, A. Sarapulova, A. Senyshyn, H. Ehrenberg, Orthomolybdates in the Cs-Fe^{II,III}—Mo–O system: Cs₄Fe (MoO₄)₃, Cs₂Fe₂(MoO₄)₃ and CsFe₅(MoO₄)₇, Eur. J. Inorg. Chem. 18 (2011) 2832–2841.
- [30] H. Ehrenberg, E. Muessig, K.G. Bramnik, P. Kampe, T. Hansen, Preparation and properties of sodium iron orthooxomolybdates, Na_xFe_y(MoO₄)_z, Solid State Sci. 8 (2006) 813–820.
- [31] P.V. Klevtsov, R.F. Klevtsova, J. Single-crystal synthesis and investigation of the double tungstates NaR³⁺(WO₄)₂, where R³⁺= Fe, Sc, Ga, and in, Solid State Chem. 2 (1970) 278–282.
- [32] S. Holbein, M. Ackermann, L. Chapon, P. Steffens, A. Gukasov, A. Sazonov, O. Breunig, Y. Sanders, P. Becker, L. Bohatý, T. Lorenz, M. Braden, Strong magnetoelastic coupling at the transition from harmonic to anharmonic order in NaFe(WO₄)₂ with 3d⁵ configuration, Phys. Rev. B 94 (2016), 104423–14.
- [33] T.M.S. Pellizzeri, C.D. McMillen, J.W. Kolis, Alkali transition—metal molybdates: a stepwise approach to geometrically frustrated systems, Chem. Eur J. 26 (2020) 597–600.
- [34] Y. Liu, L.D. Sanjeewa, V.O. Garlea, T.M.S. Pellizzeri, J.W. Kolis, A.S. Sefat, Complex magnetic order in the decorated spin-chain system Rb₂Mn₃(MoO₄)₃(OH)₂, Phys. Rev. B 101 (2020), 064423–10.
- [35] L.M. Plyasova, R.F. Klevtsova, S.V. Borisov, L.M. Kefeli, Crystal structure of iron molybdate, Dokl. Akad. Nauk USSR 167 (1966) 84–87.
- [36] A.W. Sleight, L.H. Brixner, A new ferroelastic transition in some A₂(MO₄)₃ molybdates and tungstates, J. Solid State Chem. 7 (1973) 172–174.
- [37] M.H. Rapposch, J.B. Anderson, E. Kostiner, Crystal structure of ferric molybdate, Fe₂(MoO₄)₃, J. Inorg. Chem. 19 (1980) 3531–3539.
- [38] H.Y. Chen, The crystal structure and twinning behavior of ferric molybdate, Fe₂(MoO₄)₃, Mater. Res. Bull. 14 (1979) 1583–1590.
- [39] APEX 3, v2017.3, Bruker-AXS Inc., Madison, WI, 2017.
- [40] G.M. Sheldrick, Short history of SHELX, Acta Crystallogr., Sect. A 64 (2008) 112–122.
- [41] A. Clearfield, A. Moini, P.R. Rudolf, Preparation and structure of manganese molybdates, Inorg. Chem. 24 (1985) 4606–4609.
- [42] K. Eda, Y. Uno, N. Nagai, N. Sotani, M.S. Whittingham, Crystal structure of cobalt molybdate hydrate CoMoO₄·nH₂O, J. Solid State Chem. 178 (2005) 2791–2797.
- [43] K. Eda, Y. Kato, Y. Ohshiro, T. Sugitani, M.S. Whittingham, Synthesis, crystal structure, and structural conversion of Ni molybdate hydrate NiMoO₄·nH₂O, J. Solid State Chem. 183 (2010) 1334–1339.
- [44] G. Ventruti, G.D. Ventura, M.A. Gomez, G. Capitani, M. Sbroscia, A. Sodo, Hightemperature study of basic ferric sulfate, FeOHSO₄, Phys. Chem. Miner. 47 (2020) 43
- [45] B.C. Melot, G. Rousse, J.-N. Chotard, M. Ati, J. Rodriguez-Carvajal, M.C. Kemei, J.-M. Tarascon, Magnetic structure and properties of the Li-ion battery materials FeSO₄F and LiFeSO₄F, Chem. Mater. 23 (2011) 2922–2930.
- [46] L. Skutina, E. Filonova, D. Medvedev, A. Maignan, Undoped Sr_2MMoO_6 double perovskite molybdates (M = Ni, Mg, Fe) as promising anode materials for solid oxide fuel cells. Materials 14 (2021) 1715.
- [47] M.W. Lufaso, R.B. Macquart, Y. Lee, T. Vogt, H.-C. zur Loye, Structural studies of Sr₂GaSbO₆, Sr₂NiMoO₆, and Sr₂FeNbO₆ using pressure and temperature, J. Phys. Condens. Matter 18 (2006) 8761.
- [48] B.E. Day, N.D. Bley, H.R. Jones, R.M. McCullough, H.W. Eng, S.H. Porter, P. M. Woodward, P.W. Barnes, Structures of ordered tungsten- or molybdenum-containing quaternary perovskite oxides, J. Solid State Chem. 185 (2012) 107–116.
- [49] P.F. Klevtsova, Crystal structure of the double sodium and iron molybdate NaFe (MoO₄)₂, Dokl. Akad. Nauk SSSR 221 (1975) 1322–1325.
- [50] J.-J. Li, J.-L. Zhou, W. Dong, The structure of amarillite, Chin. Sci. Bull. 35 (1990) 2073–2075.
- [51] J. Hanuza, M. Maczka, Vibrational properties of the double molybdates MX(MoO4) 2 family (M = Li,Na,K,Cs; X = Bi,Cr): Part I. Structure and infrared and Raman spectra in the polycrystalline state, Vib. Spectrosc. 7 (1994) 85–96.
- [52] J.J. Uhlrich, J. Sainio, Y. Lei, D. Edwards, R. Davies, M. Bowker, S. Shaikhutdinov, H.J. Freund, Preparation and characterization of iron molybdate thin films, Surf. Sci. 605 (2011) 1550–1555.
- [53] P. Benezeth, A. Strefansson, Q. Guatier, J. Schott mineral solubility and aqueous speciation under hydrothermal conditions to 300 °C – the carbonate system as an example, Rev. Mineral. Geochem. 76 (2013) 81–133.
- [54] M. Louvel, B. Etschmann, Q. Guan, D. Testemale, J. Brugger, Carbonate complexation enhances hydrothermal transport of rare earth elements in alkaline fluids, Nat. Commun. 13 (2022) 1456.